Ophthalmic Diagnosis and Deep Learning - A Survey

Sourya Sengupta[a,b], Amitojdeep Singh[c], Henry A. Leopold[a,b], Vasudevan Lakshminarayanan[a,b]

[a]*School of Optometry and Vision Science,University of Waterloo, Ontario,Canada*
[b]*Department of System Design Engineering,University of Waterloo, Ontario,Canada*
[c]*Birla Institute of Technology and Science Pilani, Pilani, India*

Abstract

This survey paper presents a detailed overview of the applications for deep learning in ophthalmic diagnosis using retinal imaging techniques. The need of automated computer-aided deep learning models for medical diagnosis is discussed. Then a detailed review of the available retinal image datasets is provided. Applications of deep learning for segmentation of optic disk, blood vessels and retinal layer as well as detection of red lesions are reviewed. Recent deep learning models for classification of retinal disease including age-related macular degeneration, glaucoma, diabetic macular edema and diabetic retinopathy are also reported.

Keywords: Deep Learning, Ophthalmology, Image Segmentation, Classification, Retinal Imaging

1. Introduction

In the United States, more than 40 million people are suffering acute eye related diseases that may lead to complete vision loss if left untreated [1]. Many of these diseases involve the retina. glaucoma, diabetic retinopathy and age-related macular degeneration are some of the most common retinal diseases that need proper diagnosis and treatment.

Glaucoma is one of the major causes of blindness; it is estimated that by 2020 glaucoma will attack almost 80 million people in the world [2]. The two main types of this disease are *open-angle* glaucoma and *angle closure* glaucoma. About 90% of the affected people suffer from primary open-angle glaucoma. Calculating optic cup to optic disc ratio is the most convenient way for glaucoma diagnosis. Neuroretinal rim loss, retinal nerve fibre layer

defects are also some of the measures practiced by ophthalmologists [3]. Figure 2 shows the anatomy of the retina.

The presence of diabetic retinopathy (DR) in which the retinal blood vessels get damaged is quite common for diabetes patients. It is expected that the percentage of diabetes patients worldwide will increase from 2.8% in 2000 to 4.4% in 2030. Diabetes is quite common in persons above the age of 30; uncontrolled diabetes can lead to DR [4]. Patients suffering from proliferative diabetic retinopathy (PDR) are more likely to have increased risk of diabetic nephropathy, heart attack, stroke, amputation and even death. Early stages of DR are less severe and are curable with proper clinical treatments. It is characterized by various abnormalities in retina such as microaneurysms (MA) and other small lesions caused by thin retinal capillaries breaking; these are early indicators for DR. Some of the other symptoms include hard exudates, soft exudates or cotton wool spots (CWS), hemorrhages (HEM), neovascularization (NV) and macular edema (ME) (see Figure 1) [5].

Age-related macular degeneration (AMD) is another common vision related problems. It can result in loss of vision in the middle of the visual field in the human eye, and with time there is a complete loss of central vision [6]. In the United States, almost 0.4% people from age range 50 to 60 suffer from this disease and around 12% people who are over 80 years old are affected by this disease [7].

Health-care in most countries suffers from a low doctor to patient ratio. Due to a overburdened patient-care system, diagnosis and proper treatment become error-prone and time-intensive, respectively. On the other hand, a huge amount of healthcare data is available in various medical disciplines. This data can be properly utilized by efficient computer aided diagnostics (CAD) strategies, such as feature extraction algorithms and other popular classifiers like support vector machine (SVM), artificial neural network (ANN), random forest, k-nearest neighbours etc. Computer aided detection (CADe) mainly helps a user to identify and locate a particular region of interest (ROI) in a medical image On the other hand, computer aided diagnosis (CADx) helps to analyze further about the possible outcomes of an occurrence before any manual prediction [5].

During the past few years, artificial intelligence algorithms have performed exceptionally well in classifying different types of data including images. Deep learning models are extremely powerful architectures to find patterns between different nonlinear combinations of different types of data by deriving relevant necessary representations from the data without the

requirement of manual feature extraction. In recent years, deep learning algorithms are replacing most of the traditional machine learning algorithms and in most of the cases the deep learning architectures are outperforming traditional classifiers. The advent of graphical processor unit (GPU) made application of deep learning algorithms practical and many times faster than previous CPU operations.

In retinal image analysis, the traditional CAD system architectures takes several predefined templates and kernels to compare with manually annotated and segmented parts of these images. Deep learning algorithms reportedly have showed better results than most of the popular algorithms for classification of data. General details of the different deep learning architectures can be found in the literature [8, 9]

This review describes the application of different deep learning architectures for retinal image processing and classifications found in the literature. Section 2 discusses major retina imaging techniques. Section 3 provides a short description of commonly used datasets. Section 4 reviews various applications of deep learning for detection and diagnosis problems in retinal imaging.

2. Different Retinal Imaging Techniques

2.1. Fundus Imaging Technique

Fundus imaging is the commonly used imaging technique to capture retinal images. 'Fundus' refers to the back of the pupil and fundus camera is equipped with low power microscope to capture magnified and upright view of the fundus, as shown in Figure 1. Retinal morphologies - i.e. optic disc and macula regions - and pathologies - i.e. MA - can be seen clearly in fundus images.

2.2. Optical Coherence Tomography

Optical coherence tomography (OCT) is an important technique which is used frequently in retinal image analysis, as well as in non-destructive testing and cardiology. The optical principle of OCT is based on low coherence interferometry: by applying near-infrared light, this imaging technique can capture micrometer high-resolution images [10]. Sample OCT image with labeling is shown in Figure 2.
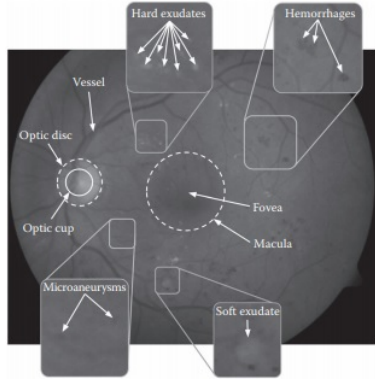
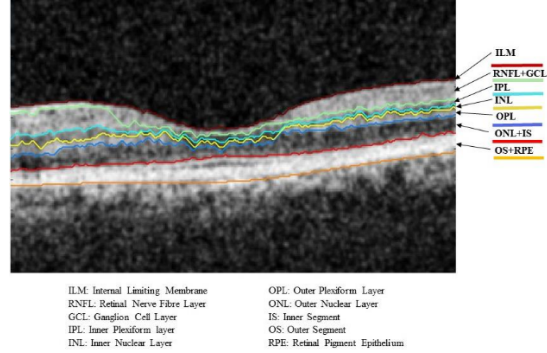Figure 1: Fundus Photograph showing retinal morphologies and pathologies [5].

Figure 2: OCT image including anatomy [10].

3. Available Datasets

The various datasets used in the literature are summarized in Table **??** and briefly described herein.

3.1. DRIVE [11]

DRIVE stands for Digital Retinal Images for Vessel Extraction. The database was obtained from a diabetic retinopathy screening program. It has 40 fundus images and among them 33 images are normal and seven images are with mild diabetic retinopathy, captured with Canon CR5 non-mydriatic 3CCD camera with a field of view (F.O.V) 45°. The dataset is available online at `https://www.isi.uu.nl/Research/Databases/DRIVE/`

3.2. HRF [12]

This public database contains 15 images of healthy patients, 15 images of patients with diabetic retinopathy and 15 images of glaucomatous patients captured with Canon CR-1 fundus camera with a F.O.V 45°. Gold standards of segmentation are provided for each image. This can be found online at `https://www5.cs.fau.de/research/data/fundus-images/`

3.3. STARE [13], [14]

Structured analysis of the retina (STARE) is a collection of 400 fundus images with blood vessel annotation on 40 images captured with TRV50 fundus camera with 35°F.O.V. The project was started on 1975 by Michael

Goldbaum at UC San Diego and funded by NIH, USA. The dataset is available online at `http://cecas.clemson.edu/~ahoover/stare/`

3.4. EyePACS [15]

This dataset is from an online competition organized by Kaggle for Diabetic Retinopathy detection. This dataset has 35126 high-resolution fundus training images and 53576 unlabelled test images. Some of the images are with no symptoms of Diabetic Retinopathy, and the others are in four groups: mild, moderate, severe, proliferative. Clinician's rating for each image is provided. This dataset is available at`https://www.kaggle.com/c/diabetic-retinopathy-detection/data`

3.5. MESSIDOR [15]

There are 1200 images in MESSIDOR dataset captured with 3 CCD camera 45°F.O.V. This retinal image dataset was created by three ophthalmologic departments funded by the French Ministry of Research and Defense. Medical experts have provided the diagnosis for retinopathy grade and macular edema risk for each image. The link for this dataset is `http://www.adcis.net/en/Download-Third-Party/Messidor.html`

3.6. ORIGA [16]

ORIGA stands for Online retinal fundus image dataset for glaucoma Analysis, and it consists of 650 retinal fundus images. The Singapore Eye Research Institute conducted the project and data were collected from the Singapore Malay Eye Study or SiMES over a three year period of 2004-2007. Online link of this dataset is `http://imed.nimte.ac.cn/en-imed-origa-650.html`

3.7. RIGA [17]

RIGA stands for Retinal fundus images for glaucoma analysis. This dataset mainly consists of retinal fundus images of glaucoma patients. Three different databases -MESSIDOR, Magrabi Eye Centre, Riyadh and Bin Rashid Ophthalmic Centre, Riyadh were concatenated to form RIGA. There are a total 760 retinal fundus images in the database. This dataset is now available online as `https://deepblue.lib.umich.edu/data/concern/generic_works/3b591905z`

3.8. DIARETDB1 [18]

This dataset consists of 84 diabetic retinopathy and 4 normal images which were acquired from Kuopio University Hospital in Finland captured with fundus camera 50°F.O.V. This dataset is online available at `http://www.it.lut.fi/project/imageret/diaretdb1/`

3.9. DIARETDB0 [19]

This database was created for benchmarking diabetic retinopathy from fundus images.There are 20 normal and 110 diabetic retinopathy images.These images were acquired from Kuopio University Hospital in Finland. Online link of the dataset is `http://www.it.lut.fi/project/imageret/diaretdb0/`

3.10. AREDS [20]

The Age-related eye disease study (AREDS) is a database with 4757 AMD and non-AMD participants collected by National Eye Institute. In Nov 2010 first part of this database came up with 72,000+ color fundus images from 595 participants. Later in 2014, 134,500+ images from 4613 participants were added to it taking the total to above 206,500. This dataset is not publicly available, but it can be obtained upon request. This dataset can be found at `https://www.ncbi.nlm.nih.gov/projects/gap/cgi-bin/study.cgi?study_id=phs000001.v3.p1`

3.11. ACHIKO-K [21]

This database is dedicated mainly for glaucoma studies and was collected from a Korean population. In this database, there are 258 manually annotated fundus images among which 114 are glaucoma images and 144 are normal images. Online link of this dataset is `https://oar.a-star.edu.sg/jspui/handle/123456789/1080?mode=full`

3.12. RIM-ONE [22]

This retinal image database is mainly focused on optic nerve head segmentation. Its initial version consists of 169 fundus images and gold standard annotations for segmentation for each image. Later on, version r2 consisting 455 images and version r3 consisting of 159 images were added.

3.13. DRISHTI-GS [23] [24]

This fundus image database is mainly for Optic Disc and Optic Cup segmentation. There are 50 training images and 51 test images in the dataset. Ground truth for each image is available in the dataset. The dataset is publicly available on `http://cvit.iiit.ac.in/projects/mip/drishti-gs/mip-dataset2/Home.php`

3.14. DRIONS-DB [25]

This database consists of 110 color fundus images. Miguel Servet Hospital, Zaragossa Spain developed this dataset for optic nerve head segmentation. Among all the patients 23.1% had chronic glaucoma and 76.9% of them had eye hypertension. This dataset can be found at `http://www.ia.uned.es/~ejcarmona/DRIONS-DB.html`

3.15. e-optha [26]

It is a color fundus dataset for Diabetic retinopathy research. This dataset has mainly two parts- one for exudates and another for Microaneurysms. There are 47 images with exudates, 35 images with no lesion, 148 images with microaneurysms, 233 images with no lesion. The full dataset is available at `http://www.adcis.net/en/Download-Third-Party/E-Ophtha.html`

3.16. Noor Hospital OCT Database [27]

This database was collected at Noor Hospital at Tehran. It consists of 50 DME, 50 normal and 48 AMD patients' OCT image data. The full dataset is available on `https://drive.google.com/file/d/1iSiFfD5LpLASrFUZu13uMFSRcFEjvbSq/view`

3.17. Heidelberg OCT database [28]

This database is for corneal OCT images taken by Heidelberg imaging device. There are 15 images mainly dedicated for layer segmentation. This dataset can be found at `https://sites.google.com/site/hosseinrabbanikhorasgani/datasets-1/corneal-oct`

3.18. OCTID [29]

This is an open-access huge OCT database with more than 500 OCT images collected from Sankara Nethralya (SN) eye hospital, Chennai, India. This database includes normal (NO), macular hole (MH), age-related macular degeneration (AMD), central serous retinopathy, and diabetic retinopathy (DR). Ground truth labels are provided for 25 images. The images will soon be available publicly.

3.19. ONHSD [30]

This fundus image database was also developed for proper optic nerve head segmentation. Ninety-nine fundus images were acquired from a diabetic retinopathy screening program. The link for this dataset is `http://www.aldiri.info/Image%20Datasets/ONHSD.aspx`

3.20. DUKE Dataset [31]

This is a recent publicly available OCT image database which consists of 269 AMD patients' images and 115 normal patients' images. The full dataset can be downloaded from `http://people.duke.edu/~sf59/RPEDC_Ophth_2013_dataset.htm`

3.21. REFUGE [32]

This dataset is part of the retinal fundus glaucoma challenge organized by Medical Image Computing and Computer Assisted Intervention 2018, Spain. This dataset has 1200 annotated fundus Images. Main task of this competition was to classify of glaucoma, segmentation of Optic Disc and cup and segmentation of fovea from the images. Recently this competition also included images for AMD. This can be found at `https://refuge.grand-challenge.org/`

3.22. UK BioBank [33]

UK Biobank is a major national and international health resource organization for health resource and it aims to improve the diagnosis and treatment of different kinds of diseases. Along with various types of medical data, the biobank has 231,806 OCT and fundus files for glaucoma, diabetic retinopathy and AMD. Website of this dataset is `https://www.ukbiobank.ac.uk`

3.23. CLEOPATRA [34]

This was a randomized study with patients with dibateic retinopathy and dibateic macular edema to investigate significance of light mask in treatment of these diseases. This study was performed in UK with 15 patients. There are total 298 total images in the dataset captured with different types of cameras.

3.24. SEED [35]

This database came out from a study performed by Singapore Epidemiology Of Eye Diseases.This dataset has 235 fundus images among which 43 are glaucoma images, 192 are normal images.

3.25. KORA [36]

The Cooperative Health Research in the Region of Augsburg developed this dataset to study AMD disease in human eye. They collected fundus images from 2840 patients. Link of this dataset is `https://epi.helmholtz-muenchen.de/`.

4. Performance Measures

Possible outcomes for any classification outcome of any sample 1. True Positive (TP): Positive sample classified as positive. 2. False Positive (FP): Negative sample classified as positive. 3. True Negative (TN): Negative sample classified as negative. 4. False Negative (FN): Positive sample classified as negative. In this section mostly used performance measures of any algorithm are discussed in brief below.

4.1. Sensitivity

This is the proportion of positive results which are classified properly as positive. Mathematically this can be written as TP/(TP+FN)

4.2. Specificity

This is the proportion of negative results which are classified properly as negative. Mathematically this can be written as TN/(TN+FP)

4.3. ROC

ROC curve, is a graphical plot between TP Rate and FP rate and Area Under Curve (AUC) means the area under the curve.It signifies the probability of a model to classify more positive than negative.

4.4. DICE Coefficient

This is the similarity index between two samples.It is also called F1 score. Mathematically it can be written as $2TP/(2TP+FP+FN)$

5. Application in Retinal Image Processing Techniques

To the best of our knowledge, the very first application of computer-aided methods to ophthalmology was by Goldbaum et al. at 1994 [37]. The authors concluded that a neural network could be trained and modeled as efficiently as trained reading to interpret visual fields of glaucoma. Another early application was the use of a neural network to predict astigmatism after cataract surgery by Severnse et al. 1993 [38]. In this section, we will discuss the more recent articles where different deep learning architectures were implemented for various ophthalmic applications.

5.1. Optic Disc Segmentation

Segmentation is an important step for automatic cropping of the region of interest for further processing. An image may possess some unwanted distortions which hamper proper processing. Noise can be present in the images and the light may not be uniform across the image. Hence for proper visualization, different parts of an image should be segmented. Over the last few years different deep learning approaches combining with various methodologies were reported to solve segmentation problems. In this section, we will be dealing with applications of different deep learning approaches to segment various morphologies of retinal images to classify and diagnose retinal diseases.

Mitra et al. [39] used CNN for ROI detection and achieved 99.05% and 98.78% accuracy on Kaggle and MESSIDOR datasets. As a data augmentation step to reduce some unwanted noise, images were divided into 13x13 grids and in each grid bounding boxes with individual class probability were given. Before training the model, k-means clustering was implemented on complete dataset. As a final step, non-maximum suppression was implemented for prediction.

Feng et al. [40] proposed unified architecture for both OD and exudates segmentation using DRIONS-DB database. FCN architecture was modified with short and long skip connections and used in this work. It achieved 93.12% Sensitivity, 99.56% specificity anf F-score of 0.9093.

Edupuganti et al. [41] used Drishti-GS dataset to implement a fully convolutional neural network (FCNN) for segmenting OD and OC for glaucoma analysis calculating the cup-to-disc ratio. Convolution was performed with a stride of 8 pixels and VGG16 encoder-decoder was implemented. Due to a limited number of image data ImageNet was used for initialization of FCN encoder. After augmentation 160 images were used for training, 10 for validation and 50 for testing. As a result highest mean accuracy achieved was 88.23%, and F scores of segmenting cup and disk were 0.897, 0.967 respectively.

Tan et al. [42] applied a 10 layer CNN on CLEOPATRA database with 149 images each for training and testing. It achieved 87.58% 71.58% sensitivity for exudates and dark lesions segmentation respectively.

Maninis et al. [43] experimented on fundus images to segment blood vessels and OD using a CNN and presented a unified deep learning based model to segment both blood vessels and optic discs together. For blood vessel segmentation authors used DRIVE and STARE, whereas for optic disc segmentation DRIONS-DB and RIM-ONE datasets were used. Taking clinician's annotations as gold standard, their frameworks were compared and as a measure of effectiveness Dice-coefficients were calculated. It was found that this method performed very similar and sometimes better than human annotations.

Lim et al. [44] proposed optic disc and optic cup segmentation for calculating cup-to-disc ratio as a measure of the presence of glaucoma using MESSIDOR and SEED-DB database. The most probable localized region around OD was chosen using Daubechies wavelet transform. Using only the red and green channel of retinal fundus images vessel masks were created to remove the obstruction of the blood vessels from the optic disc and cup. Histogram equalization was also performed on the images. Pixel level classification was performed by three-class CNN on the processed and converted image. Due to the presence of noise, probability of a pixel to be inside or outside of the OD region was calculated. This method achieved AUC 0.847.

Liu et al. [45] used monoscopic fundus images to implement deep learning based segmentation architectures to segment glaucomatous OD. The authors collected 3768 fundus images from 3 ophthalmology clinics in Australia, and from RIM-ONE and HRF. For locating and estimating size of OD difference-of-Gaussian blob detector was employed with enlarging kernel size gaussian filter to input images and pixel-wise consecutive image differences were calculated to get n-1 Gaussian maps for n input images. RestNet50 model was

implemented with 48 full convolutional neural network layers. A previously trained model with ImageNet database was used and the output layer was replaced by a new output layer with 2 nodes for 2 different classes- normal and glaucoma. For disc segmentation, 3200 images were used for training. The model achieved an accuracy of 91.6% for disc identification, with an AUC of 0.97 when applied to 800 test images. On HRF dataset it achieved 86.7% sensitivity and specificity.Overview of all the discussed literature in this section is given at Table 1.

Table 1: Summary of Some Optic Disc Segmentation Results

Reference	Modality	Architecture	Dataset	Acc	SN	SP	AUC	F1 Score
Mitra et al.	fundus	CNN	MESSIDOR, EyePACS	99.05%, 98.78%		99.14%, 98.17%		
Edupuganti et al.	fundus	VGG16 FCN	Drishti-GS					.967
Maninis et al.	fundus	CNN DRIU	DRIVE, STARE, DRIONS-DB, RIM-ONE					.822, .831, .971, .959
Lim et al.	fundus	3-class CNN	MESSIDOR, SEED-DB				.847	
Liu et al.	fundus	ResNet50 FCN	3 centres from Sydney, HRF, RIM-ONE	91.6%	87.9%	96.5%	.97	
Feng et al.	fundus	FCN	DRIONS-DB		93.12%	99.56%		0.9093

5.2. Retinal Layer Segmentation

Roy et al. [46] proposed end-to-end CNN based deep learning architecture to segment retinal layers from OCT DUKE-DME public dataset. The proposed deep learning architecture,called as ReLayNet consisted of encoder and decoder blocks followed by a classification layer. The OCT scans were width-wise sliced and the sliced data were augmented by spacial translation, horizontal flips. DICE score was used to evaluate the performance of the model and it demonstrated score of 0.94 for NFL-IPL layer, 0.9 for ILM layer, 0.87 for INL layer. The model outperformed various state-of-the-art methods for retinal layer segmentation.

Fang et al. [47] proposed a novel framework for combining CNN and graph search algorithms to segment nine different layers of OCT images. The CNN was used to extract features from the retinal boundaries initially and a classifier was trained to describe the retinal layer structures. Finally, the probability maps created from CNN outputs were used to get the final boundary layers by graph search algorithms. One hundred seventeen spectral

domain-OCT images with AMD were used to check the reliability of the model to segmentation the retinal layers from OCT images.

Pekala et al. [48] used nonproliferative diabetic retinopathy OCT images from ten patients to apply Deep Learning algorithms to the segment retinal layers. Two manual gradings were available with the dataset and among these one manual grading was taken as ground truth. A fully convolutional neural network based on DenseNet architecture was used and as post-processing step a gaussian process based regression was done. Per-pixel unsigned error was calculated using 10 fold cross validation between the ground truth and segmented image by the algorithm and the model outperformed various state-of-the-art segmentation architectures. Mean unsigned error was 1.07 with a standard deviation of 0.14.

Ben-Cohen et al. [49] reported the application of FCN to segment retinal layers of OCT images. The U-Net which is a popular architecture for image segmentation was used in this work. Graph search approach along with Sobel filtering was implemented to detect boundary layers. The algorithm was validated on 24 patients of diabetic macular edema(DME), epiretinal membrane(ERM) and achieved satisfactory results. DICE coefficients are 0.5,0.94,0.85 for 3 different FCN architectures.

Liu et al. [50] proposed a method for retinal layer segmentation from OCT images using a combination of hand-crafted features and deep features which were extracted using a deep residual network. A random forest classifier was trained using these features and at the last step shortest path was calculated to get the final segmentation from the contour probability graph of each layer obtained from the trained classifier. This method used DUKE DME dataset and achieved an F1 score of 0.885.Overview of all the discussed literature in this section is given at Table 2.

Table 2: Summary of Retinal Layer Segmentation Works

Reference	Modality	Architecture	Dataset	Acc	F1 Score
Roy et al.	OCT	FCN	DUKE		.94
Fang et al.	OCT	CNN	117 SD-OCT	1.26 mean, 1.24 SD	
Pekala et al.	OCT	FCNN	50 OCT U. of Miami	Mean error 1.1	
Ben-Cohen et al.	fundus	Patchbased U-Net FCN, OCTexplorer	TASMC(private)		.95, .94, .85(RNFL)
Liu et al.	OCT	Deep Residual Network	DUKE		.885

13

5.3. Retinal Blood Vessel Segmentation

Zhang et aL. [51] proposed a modified U-Net based architecture to segment blood vessels from fundus images of DRIVE, STARE, CHASE_DB1. By adding some additional labels on boundary areas the problem was converted into multi-class task. SGD algorithm was used to optimize model parameters. AUC of .9799 for DRIVE dataset surpassed other proposed methods' performance.

Maji et. al. [52] used ensemble of ConvNets to segment retinal blood vessels from DRIVE dataset. The networks were trained individually on the dataset of 60,000 randomly chosen 3x31x31 patches. During inference the responses are averaged to form the final segmentation. RMSProp was used as the optimizer and minibatch size of 200 was used.

Oliveira et al. [53] used DRIVE, STARE and CHASE_DB1 database to implement deep learning architecture for blood vessel segmentation. Initially, stationary wavelet transform was applied to each training image to keep multi-resolution information. A fully convolutional network was used to generate feature maps. Stochastic gradient descent with Nesterov momentum was implemented during training to decrease the cross-entropy loss function. The final probability maps for all of the image patches were merged and averaged to get a final value and thresholding was done to get the ultimate unique segmentation. An accuracy of 95.76% for DRIVE, 96.94% for STARE, 96.53% for CHASE_DB1 were achieved

Ze-Fan et al. [54] used densely Connected CNN to segment blood vessels in fundus images. A 17 layer architecture was used and the layer number X got input from the output of the previous X-1 layers and thus used the back layers of the network as features of the front layer. This model was implemented on DRIVE database and got 95% accuracy for segmenting blood vessels.

Leopold et al. [55] investigated use of CNN to segment blood vessel using standardized DRIVE dataset with RETSEG13 model and ADAM parameter optimization. The green channel of each image for classifying image pixels between vessels and non-vessel. The model gave the probability maps of every pixel to classify between vessel and non-vessel. Gabor filters were used to smooth and finalize the decision. This deep learning based architecture achieved 94.78% accuracy for classifying between these two groups.

Liskowski et al. [56] proposed a deep learning based blood vessel segmentation framework employing DRIVE, STARE and CHASE_DB1 database of

retinal fundus images. Images were standardized by subtracting the mean from every patch and dividing it with standard deviation to avoid contrast and brightness fluctuations in the image pixels. Fu et al. [57] used DRIVE, STARE, CHASE_DB1 datasets to apply deep learning for blood vessel segmentation from retinal images. Multi-scale and multi-level CNN was used and combined with conditional random field (CRF) to model the long-range interactions between pixels.It achieved an accuracy of 95.23% for DRIVE, 95.85% for STARE, 94.89% for CHASE_DB1.

Maji et. al. [58] used a hybrid of random forest and deep neural network (DNN) for blood vessel segmentation on DRIVE dataset. The DNN performed unsupervised learning of vessel dictionaties using sparse trained denoising auto-encoders (DAE). It was followed by supervised learning of random forest on the DNN response. An accuracy of 93.27% and AUC of 91.95% were achieved.

Maji et. al. [52] used ensemble of ConvNets to segment retinal blood vessels from DRIVE dataset. The networks were trained individually on the dataset of 60,000 randomly chosen 3x31x31 patches. During inference the responses are averaged to form the final segmentation. RMSProp was used as the optimizer and minibatch size of 200 was used. Maximum average accuracy of 94.7% and AUC of 92.83% was obtained. Overview of all the discussed literature in this section is given at Table 3.

Table 3: Summary of Retinal Blood Vessel Segmentation Results

Reference	Modality	Architecture	Dataset	Acc	SN	SP	AUC
Zhang et al.	fundus	CNN(U-Net)	DRIVE, STARE, CHASE_DB1	95.04%, 97.12%, 97.7%	87.23%, 76.73%, 76.7%	96.18%, 99.01%, 99.09%	.9799, .9882, .99
Oliveira et al.	fundus	CNN	DRIVE, STARE, CHASE_DB1	95.76%, 96.94%, 96.53%	80.39%, 83.15%, 77.79%	98.04%, 98.58%, 98.64%	.9821, .9905, .9855
Liu et al.	fundus	Densely Connected CNN	DRIVE	95%			
Leopold et al.	fundus	FCN using RETSEG13	DRIVE	94.78%	68.23%	98.01%	.9707
Liskowski et al.	fundus	CNN	DRIVE, STARE, CHASE_DB	97%			.99
Maji et al.	fundus	RF and DNN	DRIVE	93.27%			.9195
Maji et al.	fundus	ConvNet ensemble	DRIVE	94.7%			.9283

5.4. Red Lesion Detection

Red lesions (i.e microaneurysms and hemorrhages) in the human eye are the earliest signs of Diabetic Retinopathy. Orlando et al. [59] worked on detection of red lesions on e-ophtha, DIARETDB1 and MESSIDOR datasets

combining hand-crafted feature and deep features learned from CNN. Gaussian filtering was done to reduce unwanted noise and using linear structuring elements morphological closing was performed. It was followed by a pixel intensity thresholding operation. Deep learned feature vectors using 4 convolutional layers and 1 fully connected layers from CNN(trained using LeNet architecture) were formed combining handcrafted features drawn from the green channel of the normalized and equalized image. Due to the presence of per lesion level annotations, e-optha and DIARETB1 were used for per-lesion performance detection. For the two different experiments, i.e small red lesion detection and lesion with multiple sizes detection, AUC for e-optha and MESSIDOR were 0.8812 and 0.8932, respectively.

Grinven et al.[60] proposed a methodology to detect hemorrhages in retinal fundus images by classifying lesions. MESSIDOR and EyePACS datasets were employed. As pre-processing steps, circular Field of View was extracted and images were resized, and contrast enhanced. Pixel values were extracted for both with hemorrhage and without hemorrhage cases for training purpose. CNN architecture inspired by OxfordNet was implemented and to efficiently design the training framework selective sampling algorithm [61] was introduced to perform iteratively and it enhanced the performance by decreasing the number of epochs from 170 to 60. CNN with selective sampling was found to decrease the time of epochs and also to enhance the AUC to a value of 0.972 which is better than CNN with no selective sampling with a value of 0.894.

Lam et al. [62] used a deep learning architecture to detect the presence of five classes of red lesions i.e. normal, microaneurysms, hemorrhages, exudates, retinal neovascularization in EyePACS Dataset. The CNN was trained with 1050 images using GoogleNet architecture. This model was evaluated using e-ophtha dataset. Patches were extracted with varying shapes and sizes according to the size of the lesions. 609 abnormal and 576 normal images were extracted from 243 whole images. For testing, a sliding window was introduced to make a full scan over the whole image by the CNN to give a multiclass outcome probability. The model achieved maximum 98% patch classification accuracy which is similar in GoogLeNetV1, ResNet, VGG16, AlexNet and InceptionV3.

Shan et al. [63] employed transfer learning approach using stacked sparse autoencoder(SSAE) with 89 retinal fundus images DIARETDB dataset to classify between MA and non-MA patches. Image patches were passed through SSAE to obtain features and softmax layer was used to classify

the labels. In terms of accuracy this method obtained 91.38%, this method also obtained specificity of 91.6%.

Haloi [64] used a 5 layer CNN network to detect Microaneurysm (MA) in MESSIDOR and Retinopathy Online Challenge (ROC) datasets.The method achieved sensitivity of 97%, specificity of 96%, accuracy of 96% and AUC of 98.8% on Messidor dataset whereas it had an AUC of 98% on ROC dataset.Overview of all the discussed literature in this section is given at Table 4.

Table 4: Summary of Red Lesion Detection Works

Reference	Modality	Architecture	Dataset	Acc	SN	SP	AUC
Orlando et al.	fundus	CNN using LeNet architecture	e-optha, MESSIDOR				.8812, .8932
Grinsven et al.	fundus	CNN using OxfordNet	MESSIDOR, EyePACS		91.9%, 83.7%	91.8%, 85.1%	.972, .895
Lam et al.	fundus	CNN using GoogleNet3	EyePACS, e-optha	98%			.95
Shan et al.	fundus	Transfer Learning (SSAE)	DIARETDB	91.38%			.916
Haloi	fundus	5 layer CNN	MESSIDOR, ROC	96%	97%	96%	.982, .98

5.5. Disease Classification

5.5.1. Age-relatad Macular Degenration- AMD

Grassmann et al. [65] proposed a deep learning based classification architecture to predict the severity of AMD in the human eye. In this work, an ensemble of several convolutional neural networks was used to classify among 13 different classes of AMD i.e. 9 AREDS steps [66] , 3 late AMD, 1 class of ungraded images. Mainly there are four different steps can be found in this methodology. Firstly, for color balance and illumination correction some preprocessing steps were done. Then 6 different neural networks (AlexNet, GoogLeNet, VGG, ResNet, Inception-v3, 1-ResNet-v2) were used independently to train the model. With the result obtained from each of the individual neural networks, a random forest ensemble model was developed. This complete model is then applied to predict classes of severity to AREDS data and KORA data and achieved decent accuracy with a quadratic weight of 0.95.

Horta et al. [67] reported a hybrid method- frame employing deep image features and random forest to combine different patient non-visual data like lifestyle, cataract, demographics with the image for classification. Detection of the circular boundaries of the retina, normalization of intensity level,

17

lightness channel extraction from L*a*b color space and finally resizing the image for changing the resolution was done as preprocessing steps. Next, to extract deep image features, CNN (pre-trained with 1.2 million image data) was used. The deep features combined with the non-medical non-visual information of the patients were used to train a Random Forest Classifier to perform binary classification for higher severity AMD and lower severity of AMD. The combined features were found to achieve higher accuracy than individual feature set with an AUC 84.76% and accuracy of 79.04%.

Burlina et al. [68] used a combination of universal deep features and transfer learning approach for classification of different AMD classes. After pre-processing, 4096 deep features from Overfeat [69] were extracted and Linear SVM was employed at last step for final classification. In this work, AREDS dataset with 5664 images is used, and 4-class, 3-class, 2-class classifications were done and compared with a human physician and achieved highest of 93.4% accuracy for 2-class classification which is quite close to human physician accuracy of 95.2%.

Burlina et al. [70] used a completely data-driven approach using deep CNN (DCNN-A) to perform a binary classification between early-stage AMD and advanced stage AMD using the same AREDS database with almost 130000 images. The AlexNet model was implemented in this work using Keras and Tensorflow. This method was compared with the previous methods combining both Deep Features, transfer learning and DCNN-A achieved a classification accuracy of 91.6% which is greater than human accuracy.

Govindaiah et al.[71] reported an extended study of previous work on AREDS fundus AMD dataset using a modified VGG16 architecture. Macula was chosen as a Region of Interest and images were resized to a common reference level. For classification, a modified VGG16 architecture was implemented using 3x3 convolution layer and 2x2 pooling layer and for comparison a 50 layer Keras implementation of residual neural network was used. This architecture gave an accuracy of upto 92.5% in binary classification between no/early stage AMD and intermediate/advanced stage AMD.

Matsuba et al. [72] published an approach for detecting AMD disease from ultra wide-range color fundus images.In this work, 227 normal images and 137 AMD images from Tsukazaki Hospital were used. The accuracy of DCNN in this area was used and compared with human grading by six opthalmologists and an average AUC of 99.76% was reported. Three convolutional layers, with ReLU unit and Max-pooling layers are used to perform this experiment on pre-processed fundus images.

Tan et al.[73] used fundus images and implemented a deep learning algorithm to detect AMD. A fourteen layer CNN was used to get an accuracy of 91.17% and 95.45% respectively for blindfold and ten-fold cross-validation. In this work, 402 normal fundus images, 583 intermediate AMD fundus images and 125 wet AMD images from Kasturba Medical College (KMC), Manipal, India were used. Three fully-connected layers, 4 max-pooling layers, and 7 convolutional layers were implemented in this work. Adam optimization [74] was used for tuning the CNN model's parameters.

Treder et al. [75] presented an application of Deep Learning in spectral domain OCT image (SD-OCT) classification for AMD detection. SD-OCT data from 701 AMD and 311 healthy patients were used for this multi-layer Deep CNN classification model. In an Inception-v3 network, the first layer was modeled as DCNN trained with millions of images and the last layers were trained with SD-OCT images for performing classification. After the first 500 steps, this model achieved an accuracy of 100%.

Kermany et. al [76] used TensorFlow Platform to apply transfer learning on 51,140 normal, 8,617 drusen, 37,206 choroidal neovascularization and 11,349 diabetic macular edema images. The model is applied to 1000 untrained OCT images for validation. It achieved a 100% accuracy for classification between normal and choroidal neovascularization images whereas it was able to classify between diabetic macular edema and normal images with 98.2% accuracy, and between normal and drusen images with 99% accuracy.Overview of all the discussed literature in this section is given at Table 5.

5.5.2. Glaucoma

Deep learning has been extensively applied for glaucoma diagnosis achieving good results on various fundus and OCT datasets. Asoaka et al. [77] used a 3 layer deep Feed-forward Neural Network (FNN) on a dataset of 171 Glaucoma images. It achieved an AUC of 92.6% performing better than traditional machine learning techniques.

Zhixi et al. [78] used Inception-v3 architecture on a large database with 48,000+ images to detect glaucomatous optic neuropathy. The images were graded by 21 licensed ophthalmologists and reference standard was made until 3 graders agreed. Local space average color subtraction was applied in pre-processing to accommodate for varying illumination. Inception-v3 network was used for classification. The large dataset in conjunction with a deep model provides good results with an AUC of 98.6%.

Table 5: Summary of AMD Detection Works

Reference	Modality	Architecture	Dataset	Acc	SN	SP	AUC
Grassmann et al.	fundus	CNN using AlexNet, GoogleNet, VGG, ResNet, Inception-v3, 1-ResNet-v2	AREDS and KORA	94.3%			
Horta et al.	fundus	DCNN	AREDS	79.04%	66.34%	88.95%	.8476
Burlina et al.	fundus	Deep Features with SVM	AREDS	93.4%			
Burlina et al.	fundus	DCNN using AlexNet	AREDS	91.6%			.96
Govindaiah et al.	fundus	VGG16	AREDS dataset	92.5%			
Matsuba et al.	fundus	DCNN	Tsukazaki Hospital	100%	100%	97.31%	.9976
HongTan et al.	fundus	CNN	Kasturba Medical College	95.45%	96.43%	93.45%	
Treder et al.	SD-OCT	701 AMD, 311 healthy	CNN using Inception-v3	96%	100%	92%	
Kermany et al.	OCT	Transfer Learning	51140 normal, 8617 drusen, 37206 CNV, 11349 DME	96.6%	97.8%	97.4%	.999

Chen et al.[79] implemented a CNN with dropout and data augmentation on ORIGA and SCES dataset. A six layers deep CNN with 4 convolutional layers of progressively decreasing filter size (11, 5, 3, 3) followed by 2 dense layers was used to get 83.1% and 88.7% AUC on ORIGA and SCES respectively.

In a later work, Chen et al[80] presented a model using Contextualized CNN (C-CNN) architecture. Multilayer perceptron convolutional layer was used due to its compatibility with CNN during back-propagation and for adding depth to the model. It combined the output of convolutional layers of multiple CNN to a final dense layer to obtain the softmax probabilities. 5 C-CNN model which was a concatenation of outputs of last Convolutional layers of 5 CNNs each of depth 6 (5 convolutional layers + 1 MLP) provided AUC of 83.8% and 89.8% on ORIGA and SCES datasets, respectively.

Chai et al.[81] presented a model which took- disk image, whole image and domain knowledge features. The disk image provided local CNN features, the whole image provided global CNN features whereas domain knowledge features were obtained from diagnostic reports. It used a total of 25 features

including 3 numerical features- intraocular pressure, age, and eye sight as well as 22 binary features like swollen eye, headache, eye hurts, blurred vision and failing eyesight. The disk and whole images were fed to two separate CNN while domain knowledge features were fed to a third branch consisting of a fully connected neural network. These three branches were concatenated by a merge layer followed by two dense layers and logistic regression classifier. The model benefited from diagnostic features along with fundus images and attained an accuracy 91.51% .

Fu et al. [82] presented DENet architecture combined global fundus image with local optic disk area. The network was made up of four streams of of information. The first global stream classified the entire fundus image directly using a pre-trained ResNet 50 model. The second global stream used a segmentation based network to localize optic disk for detection and was based on U-net architecture. It had an extended branch from the smallest size and highest number of channels part of U-net for detection. The first optic disk level stream used ResNet on local disk area, whereas polar coordinate transformed disc area was used in the second stream. Enlargement of the concentric disk and cup circles and equivariance for data augmentation were cited as advantages of polar transformation. The combination of the 4 streams was ensembled to obtain the final result for predicting glaucoma giving an accuracy of 83.2% on SCES and 66.6% on SINDI datasets.

Chakravarty [83] used a multi-task CNN based on U-net for joint segmentation of OD, OC and glaucoma prediction from fundus pictures. CNN feature sharing for different tasks ensured better learning and over-fitting prevention. The parts of the model that were shared with U-net contained 8 times less number of CNN filters than the U-net. It was most likely done to prevent over-fitting since the study used a smaller dataset than U-net. It used an encoder network to downsample the feature and then a decoder network to restore the image size. Two different convolutional layers were applied on the decoder network's output for OC and OD segmentation. The OC and OD segmentation masks were merged into separate channels and CNN was applied on it. The outputs of the CNN and encoder output were combined and fed to a single neuron to predict glaucoma achieving an AUC of 94.56%.

Muhammad et al. [84] used a hybrid of AlexNet and random forest on wide field OCT of 102 patients for glaucoma classification. The pre-trained AlexNet model was used for feature extraction from OCT images. The weights of nodes of fully connected layers of the neural net were used as

Table 6: Summary of Glaucoma Detection Works

Reference	Modality	Architecture	Dataset	Acc	SN	SP	AUC
Asoaka et al.	fundus	3 layer FNN	Private: 171				.926
Zhixi et al.	fundus	Inception-v3	Private:48000+		95.6%	92.0%	.986
Chen et al.	fundus	4 layer CNN	ORIGA, SCES				.831, .887
Chen et al.	fundus	C-CNN	ORIGA, SCES				.838, .898
Chai et al.	fundus	MB-NN	Private: 2554	91.51%	92.33%	90.90%	
Fu et al.	fundus	DENet	SCES, SINDI	83.2%, 66.6%		70.67%, 37.53%	
Chakravarty et al.	fundus	Multi-task CNN	REFUGE				.95
Muhammad et al.	OCT	HDLM	Private:102 images	93.1%			
Fu et al.	OCT	MCDN	Private:8270 images	89.26%	88.89%	89.63%	.9456

input for the random forest classifier. The classifier had 200 trees and the method was repeated for 50 times taking the average for the results. Six image types for each patient were used with leave-one-out cross-validation to train the model. A vertically flipped copy of each image was also added and nodes from Fully Connected layer 6 were found to have the best accuracy of 93.1% using RNFL probability map(4). The method outperforms OCT and VF clinical metrics which gave upto 87.3% accuracy but fell short of 98% obtained by an experienced human expert.

Fu et. al. [85] presented multi-context deep network (MCDN) for angle-closure glaucoma screening using anterior segment Optical Coherence Tomography (AS-OCT) imagery. The network used data from the local window and global image as well as patient data to classify between Open-angle and Angle-closure glaucoma using a dataset of 8270 images. Two parallel streams were used to perform fine-tuning on pre-trained VGG-16 on the local and global image. The feature maps from these streams were concatenated at the dense layer and supplemented with clinical parameters analyzed by a linear SVM for final classification. Intensity-based data augmentation was performed instead of traditional scale based augmentation because the anterior chamber was found at a consistent position in AS-OCT images. The performance was incrementally analyzed using various combinations of the three input streams and the combined MCDN was found to obtain the best AUC of 0.9456. Overview of all the discussed literature in this section is given at Table 6.

5.6. Diabetic Macular Edema(DME)

Chan et al. [86] performed transfer learning with OCT images collected from Singapore Eye Research Institute and the Chinese University Hong Kong to perform classification between normal and diabetic macular edema. Features collected from preprocessed images with ALexNet, VggNet, GoogleNet were combined to form feature vector. Dimension was reduced using PCA algorithm. KNN, SVM, Random Forest classifiers were used and with the majority voting between the classifiers highest accuracy and SP were 90.63% and 93.75% respectively.

Vahadan et al. [87] used patch based deep learning architecure for detecting diabetic macular edema by two step methods using Heidelberg OCT image data. In first step using image processing techniques were used to extract hard exudates, fluid filled region, retinal pigment epithelium. Then patch based CNN classifier was used to determine if the class was with DME or not. It achieved an F1 score of 0.9281 on the test dataset.

Varadarajan et al. [88] used Inception-v3 CNN architecture to train a model to predict presence of diabetic macular edema. Model was trained with fundus photograph and corresponding OCT images were used for testing. 6039 images collected from Rajavithi Hospital Thailand were used to train the model and finally AUC was 0.89 , Sensitivity was 0.85, Specificity 0.8.

Perdomo et al. [89] presented end-to-end CNN architecture to classify diabetic macular edema and normal OCT images. Authors achieved 93.75% accuracy with a margin of error 3.125%. 12 layer CNN was used after preprocessing (cropping and resizing) the images. The Singapore Eye Research Institute (SERI) database with 32 volumes spectral domain OCT images were used for this work.Overview of all the discussed literature in this section is given at Table 7.

Table 7: Summary of DME Detection Works

Reference	Imaging Modality	Architecture	Dataset	Acc	SN	SP	AUC	F1 Score
Chan et al.	OCT	CNN features+ Majority voting	SERI	93.75%	93.75&	93.75%		
Vahadan et al.	OCT	patchbased CNN	Heidelberg					0.9281
Varadarajan et al.	OCT	Rajavithi Hospital Thailand	CNN Inception v-3	85%	80%	89%		
Perdomo et al.	OCT	SERI	CNN	93.75%				

5.6.1. Diabetic Retinopathy

In this section different applications of deep learning algorithms for diabetic retinopathy detection are described briefly.

Gargeya et al.[90] reported a deep learning architecture to classify between normal and DR fundus images. Using the principle of deep residual learning, CNN model was built to learn deep discriminative features for detecting DR. From average pooling layer of CNN, 1024 features were yielded. Metadata analysis was introduced to increase the accuracy and hence metadata features related to 3 metadata variables i.e. pixel height, pixel width and field of view of the image were appended to form a final feature vector with 1027 features. A second level tree-based gradient boosting classifier was designed and implemented on EyePACS dataset. With a sensitivity and specificity of 94% and 98%, the model achieved AUC of 0.97.

Takahashi et al. [91] graded different stages of the presence of DR using GoogleNet architecture and achieved a mean accuracy of 96% Among 9939 posterior pole images, 496 images were included for validation and all other images were used for training the model. The model was designed using two different ways, first with manual staging of three color photographs (AI1) and second with manual staging of only one color photograph. (AI2) From the GoogleNet model- 5 top layers were deleted, crop size was expanded , batch size was reduced. 20 fold cross-validation was used and for comparison AI1 was also trained with ResNet model. For AI1 the mean accuracy achieved was 81% but for AI2 it was 77%. The final mean accuracy for 20 fold cross validation was 80%.

Using a retinal fundus image dataset consists of 70000 images, Colas et al. [92] proposed a DR grading method. There were 4 different classes of DR images in the dataset- no DR, mild DR, moderate DR and acute DR. The trained model was tested on Kaggle DR detection competition database of 10000 fundus images collected from 5000 patients. This DR grading algorithms achieved 94.6% area under the cure with a sensitivity of 96.2% and 66.6% specificity.

García et.al [93] applied different architectures of CNN for DR detection using the EyePACS, achieving an accuracy of 83.68%. As a pre-processing step, images were subtracted from color mean and rescaled to 256x256. Data augmentation by flipping the images was done for increasing the robustness. Several neural network architectures using various learning rates and different number of layers were used to test the highest accuracy. The model after 90

epochs achieved the highest accuracy of 83.68 %

Abràmoff et. al [94] described DR detection with real-time data using a device called IDx-DR X2.1. This device applied a CNN inspired from AlexNet models to retinal images to and classify different types of DR and achieved a sensitivity of 96.8% and specificity of 87%. Main classes of diseases were referable DR(rDR), vision-threatning DR(vtDR), proliferative DR(Pdr). The CNN-based architectures were designed to characterize and detect optic disc, fovea and lesion characteristics. The sensitivity of rDR detection with rDR output using the device was 96.8%. The device's rDR output to detect and locate vtDR has a result of 100 % AUC and rDr checking with rDr index achieved AUC of 98%.

Brown et. al [95] performed a vessel segmentation using U-Net deep learning architecture and classification of premature retinopathy disease using GoogleNEt architecture. Initially, as pre-processing step images were resized to 640x480 pixels. GoogleNet Inception v-1 architecture was trained with a learning rate of 0.0001 to produce three different class outputs of premature retinopathy such as normal, pre-plus, plus and severity score was calculated using the probability of each class. The t-distributed stochastic neighbor embedding was used to visualize high dimensional CNN features to a two-dimensional space. ROC of 0.98 was achieved for plus disease vs normal.

Gulshan et al. [96] used deep learning algorithms to identify presence of diabetic retinopathy using EyePACS dataset and images from 3 eye hospitals in india, EyePACs-1 and MESSIDOR-2 dataset. Five different types of DR and presence of macular edema were graded by expert clinicians. Inception v-3 model was used, stochastic gradient descent algorithm was implemented for optimization and with the weights of the pre-trained model with ImageNet data batch normalization was done. To evaluate the performance of the model Sensitivity, Specificty and AUC were used such as in the case of referable DR the model gave sensitivity of 90.3% and 87%, specficity of 98.1% and 98.5%, AUC of 0.991 and 0.990 respectively for EyePACS-1, Messidor-2.

Quellec et al. [97] discussed a method to detect referable DR as well as Lesions with ConvNet architecure using o_O Solution [98]. This proposed model was mainly based on visualization methods of CNN. Heatmap generation modifications were proposed in this purpose to jointly improve the quality of DR and lesion detection.Kaggle 2015, DiaretDB1, e-optha datasets were used and AUC achieved were 0.954, 0.955, 0.949 respectively.Overview of all the discussed literature is given at Table 8.

Table 8: Summary of Diabetic Retinopathy Detection Works

Reference	Modality	Architecture	Dataset	Acc	SN	SP	AUC
Gargeya et al.	fundus	CNN Deep Residual Learning	EyePACS, MESSIDOR e-Optha2		94%	98%	.97
Takahashi et al.	fundus	CNN GoogleNet, ResNet	9839 images	96%			
Colas et al.	fundus	CNN	EyePACS		96.2%	66.6%	.946
Garcia et al.	fundus	CNN AlexNet	EyePACS	83.68%		93.65%	
Abramoff et al.	fundus	CNN AlexNet	Messidor-2		96.8%	87%	
Brown et al.	fundus	CNN GoogleNet, U-Net, Transfer Learning	Private: 6000 images		96.8%	87%	.98
Gulshan et al.	fundus	CNN Incetionv-3	EyePACS-1, Messidor-2		90.3%, 87%	98.1%, 98.5%	.99, .99
Quellec et al.	fundus	ConvNet	Kaggle, e-optha, DiaretDB1				.954, .949, .955

6. Discussions

This review tries to address different kinds of applications of deep learning methodologies in ophthalmic diagnosis.Previous reviews published in this domain were very much clinical, focused on traditional machine learning algorithms or narrowly focused on a particular disease or focused on hardware implementation of artificial intelligence in ophthalmic diagnosis [99][100][101][102]. None of them covered detailed reviews of different state-of-the art deep learning algorithms used for various ophthalmic diagnosis. Hence, to the best of our knowledge this is the first thorough and detailed review article of deep learning algorithms and performance outcomes of different architectures for ophthalmic diagnosis by retinal image processing techniques.

It is quiet prominent from the survey that deep learning applications in retinal images are quite useful and effective. It reduces the need of manual feature extraction as the methodologies are mainly data-driven. CNN was the most widely used architecture for classification, detection or segmentation of different parts of fundus or OCT images. FCN, Deep Residual Network, Densely Connected Neural Network, Transfer Learning, and AE based architectures were also reported. In many cases, proposed deep learning frameworks surpassed prior traditional state-of-the-art methods.

Deep learning is a data-driven approach hence need of large amount of annotated medical data is required to develop a robust model. The availability

of large amount of data reduces over-fitting and helps the model to generalize the pattern. But still there is no such huge publicly available datasets in the domain of retinal imaging. This is especially prominent in detection problems where the labels are at a image level. For example there are no studies on a very large standardized public dataset in case of glaucoma, many datasets were even private, which makes the quantitative comparison between techniques impossible. In segmentation problems the pixel wise labels along with patching alleviate this issue greatly, leading to reliably comparable results on small datasets like DRIVE. As an example, for AMD detection, Grassmann et al.[65] used CNN to achieve an accuracy of 94.3% and it surpassed most of the state-of-the-art algorithms on AREDS dataset, but overall Matsuba et al.[72] achieved 100% accuracy and 100% sensitivity with Tsukazaki Hospital dataset. Here Matsuba et al. didn't use any publicly available dataset, hence it is quite ambiguous to declare the best methodologies for a particular work. The release of large publicly available standard datasets for retinal disease detection is essential for growth of this area. Focus should be given on making a robust model to handle variations arising from different patient demographics and imaging equipment.

Another problem is the unavailability of standardized KPIs (Key Performance Indicators) for measuring the performance of a particular model. Different researchers used different indices to measure their work. Hence it is hard to compare between different deep learning architectures for a particular area. For a given model, it is very rare to get best results in terms of all the performance measures compared to other methods. For example, in lesion detection works, Lam et al. [62] achieved accuracy of 98% which is higher than most of the other state-of-the-art methods, whereas in terms of AUC Haloi[64] achieved 0.982 which is higher than other reported AUCs. Leopold et al.[103] approached this issue while reporting the results and also reported more generalized metrics like G-mean and MCC to measure a model's effectiveness.

7. Future Research

In most of the works, data for both training and testing were extracted from same dataset, but in real world it is not always possible to get test data and training data from same distribution. Hence the model should be robust enough to deal with data from a different distribution for testing purpose. This field is called domain adaptation- more focus should be given

on deep domain adaptation approaches to make completely robust model which can be implemented for real case scenario.Wang et al. [104] discussed different deep domain adaptation algorithms which can be used to address this problem. In the context of ophthalmic diagnosis this can be an important direction for future research.

8. Acknowledgement

References

[1] J. P. Whitcher, M. Srinivasan, M. P. Upadhyay, Corneal blindness: a global perspective, Bulletin of the world health organization 79 (2001) 214–221.

[2] C. Costagliola, R. Dell'Omo, M. R. Romano, M. Rinaldi, L. Zeppa, F. Parmeggiani, Pharmacotherapy of intraocular pressure: part i. parasympathomimetic, sympathomimetic and sympatholytics, Expert opinion on Pharmacotherapy 10 (16) (2009) 2663–2677.

[3] M. Nicolela, J. Vianna, Optic nerve: clinical examination (2016) 17–26.

[4] A. Krolewski, J. Warram, L. Rand, A. Christlieb, E. Busick, C. Kahn, Risk of proliferative diabetic retinopathy in juvenile-onset type i diabetes: a 40-yr follow-up study, Diabetes care 9 (5) (1986) 443–452.

[5] H. Leopold, J. Zelek, V. Lakshminarayanan, Deep learning methods for retinal image analysis.

[6] R. Jager, W. Mieler, J. Miller, Age-related macular degeneration, New England Journal of Medicine 358 (24) (2008) 2606–2617.

[7] D. Friedman, B. O'Colmain, B. Munoz, S. Tomany, D. J. P. N. B. M. P. K. J. McCarty, C, et al., Prevalence of age-related macular degeneration in the united states, Arch ophthalmol 122 (4) (2004) 564–572.

[8] Y. LeCun, Y. Bengio, G. Hinton, Deep learning, nature 521 (7553) (2015) 436.

[9] Y. Guo, Y. Liu, A. Oerlemans, S. Lao, S. Wu, M. S. Lew, Deep learning for visual understanding: A review, Neurocomputing 187 (2016) 27–48.

[10] P. Roy, Automated segmentation of retinal optical coherence tomography images, Master's thesis, University of Waterloo (2018).

[11] J. Staal, M. Abràmoff, M. Niemeijer, M. Viergever, B. Van Ginneken, Ridge-based vessel segmentation in color images of the retina, IEEE transactions on medical imaging 23 (4) (2004) 501–509.

[12] A. Budai, R. Bock, A. Maier, J. Hornegger, G. Michelson, Robust vessel segmentation in fundus images, International journal of biomedical imaging 2013.

[13] A. Hoover, V. Ko, M. Goldbaum, Locating blood vessels in retinal images by piecewise threshold probing of a matched filter response, IEEE Transactions on Medical imaging 19 (3) (2000) 203–210.

[14] A. Hoover, M. Goldbaum, Locating the optic nerve in a retinal image using the fuzzy convergence of the blood vessels, IEEE transactions on medical imaging 22 (8) (2003) 951–958.

[15] M. Niemeijer, B. Van G, M. Cree, A. Mizutani, G. Quellec, C. Sánchez, B. Zhang, R. Hornero, M. Lamard, C. Muramatsu, et al., Retinopathy online challenge: automatic detection of microaneurysms in digital color fundus photographs, IEEE transactions on medical imaging 29 (1) (2010) 185–195.

[16] Z. Zhang, F. Yin, J. Liu, W. Wong, N. Tan, B. Lee, J. Cheng, T. Wong, Origa-light: An online retinal fundus image database for glaucoma analysis and research, in: Engineering in Medicine and Biology Society (EMBC), 2010 Annual International Conference of the IEEE, IEEE, 2010, pp. 3065–3068.

[17] A. Almazroa, S. Alodhayb, E. Osman, E. Ramadan, M. Hummadi, M. Dlaim, M. Alkatee, V. Lakshminarayanan, Retinal fundus images for glaucoma analysis: the riga dataset, in: Medical Imaging 2018: Imaging Informatics for Healthcare, Research, and Applications, Vol. 10579, International Society for Optics and Photonics, 2018, p. 105790B.

[18] T. Kamarainen, L. Sorri, A. Pietilä, H. Uusitalo, the diaretdb1 diabetic retinopathy database and evaluation protocol, in: Proceedings of British Machine Vision Conference, 2007.

[19] T. Kauppi, V. Kalesnykiene, J. Kamarainen, L. Lensu, I. Sorri, H. Uusitalo, H. Kälviäinen, J. Pietilä, Diaretdb0: Evaluation database and methodology for diabetic retinopathy algorithms, Machine Vision and Pattern Recognition Research Group, Lappeenranta University of Technology, Finland 73.

[20] T. Clemons, E. Chew, S. Bressler, W. McBee, Age-related eye disease study research, g. national eye institute visual function questionnaire in the age-related eye disease study (areds): Areds report no. 10, Arch Ophthalmol 121 (2) (2003) 211–7.

[21] Z. Zhang, J. Liu, F. Yin, B. Lee, D. Wong, K. Sung, Achiko-k: Database of fundus images from glaucoma patients, in: 2013 IEEE 8th Conference on Industrial Electronics and Applications (ICIEA), IEEE, 2013, pp. 228–231.

[22] F. Fumero, S. Alayón, J. Sanchez, J. Sigut, M. Gonzalez-Hernandez, Rim-one: An open retinal image database for optic nerve evaluation, in: 2011 24th international symposium on computer-based medical systems (CBMS), IEEE, 2011, pp. 1–6.

[23] J. Sivaswamy, S. Krishnadas, A. Chakravarty, G. Joshi, A. Tabish, et al., A comprehensive retinal image dataset for the assessment of glaucoma from the optic nerve head analysis, JSM Biomedical Imaging Data Papers 2 (1) (2015) 1004.

[24] J. Sivaswamy, S. Krishnadas, G. Joshi, M. Jain, A. Tabish, Drishtigs: Retinal image dataset for optic nerve head (onh) segmentation, in: 2014 IEEE 11th International Symposium on Biomedical Imaging (ISBI), IEEE, 2014, pp. 53–56.

[25] E. Carmona, M. Rincón, J. García-Feijoó, J. Martínez-de-la Casa, Identification of the optic nerve head with genetic algorithms, Artificial Intelligence in Medicine 43 (3) (2008) 243–259.

[26] E. Decencière, G. Cazuguel, X. Zhang, G. Thibault, J.-C. Klein, F. Meyer, B. Marcotegui, G. Quellec, M. Lamard, R. Danno, et al.,

Teleophta: Machine learning and image processing methods for teleophthalmology, Irbm 34 (2) (2013) 196–203.

[27] R. Rasti, H. Rabbani, A. Mehridehnavi, F. Hajizadeh, Macular oct classification using a multi-scale convolutional neural network ensemble, IEEE transactions on medical imaging 37 (4) (2018) 1024–1034.

[28] M. Jahromi, R. K, H. Rabbani, A. Dehnavi, A. Peyman, F. Hajizadeh, M. Ommani, An automatic algorithm for segmentation of the boundaries of corneal layers in optical coherence tomography images using gaussian mixture model, Journal of medical signals and sensors 4 (3) (2014) 171.

[29] M. P. V. L. P Gholami, P Roy, Octid: Optical coherence tomography image database.

[30] J. Lowell, A. Hunter, D. Steel, A. Basu, R. Ryder, E. Fletcher, L. Kennedy, et al., Optic nerve head segmentation, Medical Imaging, IEEE Transactions on 23 (2) (2004) 256–264.

[31] S. Farsiu, S. Chiu, R. O'Connell, F. Folgar, E. Yuan, J. Izatt, C. Toth, A.-R. E. D. S. . A. S. D. O. C. T. S. Group, et al., Quantitative classification of eyes with and without intermediate age-related macular degeneration using optical coherence tomography, Ophthalmology 121 (1) (2014) 162–172.

[32] Retinal fundus glaucoma challenge.

[33] D. Mitry, T. Peto, S. Hayat, J. Morgan, K. Khaw, P. Foster, Crowdsourcing as a novel technique for retinal fundus photography classification: Analysis of images in the epic norfolk cohort on behalf of the ukbiobank eye and vision consortium, PloS one 8 (8) (2013) e71154.

[34] S. Sivaprasad, G. Arden, A. Prevost, R. Crosby-Nwaobi, H. Holmes, J. Kelly, C. Murphy, G. Rubin, J. Vasconcelos, P. Hykin, A multicentre phase iii randomised controlled single-masked clinical trial evaluating the cl inical e fficacy and safety of light-masks at p reventing dark-a daptation in the tr eatment of ea rly diabetic macular oedema (cleopatra): study protocol for a randomised controlled trial, Trials 15 (1) (2014) 458.

[35] Y. Zheng, C.-Y. Cheng, E. L. Lamoureux, P. Chiang, A. Anuar, J. Wang, P. Mitchell, S. Saw, T. Wong, How much eye care services do asian populations need? projection from the singapore epidemiology of eye disease (seed) study, Investigative ophthalmology & visual science 54 (3) (2013) 2171–2177.

[36] C. Brandl, V. Breinlich, K. Stark, S. Enzinger, M. Aßenmacher, M. Olden, F. Grassmann, J. Graw, M. Heier, A. Peters, et al., Features of age-related macular degeneration in the general adults and their dependency on age, sex, and smoking: results from the german kora study, PloS one 11 (11) (2016) e0167181.

[37] M. Goldbaum, P. Sample, H. White, B. Colt, P. Raphaelian, R. Fechtner, R. Weinreb, Interpretation of automated perimetry for glaucoma by neural network., Investigative ophthalmology & visual science 35 (9) (1994) 3362–3373.

[38] M. Severns, V. Lakshminarayanan, P. Smith, Predicting astigmatism after cataract surgery using a neural network, Visual Optics/Noninvasive Assessment of the Visual System Technical Digest, (1993) 3:34–37.

[39] A. Mitra, P. Banerjee, S. Roy, S. Roy, S. Setua, The region of interest localization for glaucoma analysis from retinal fundus image using deep learning, Computer methods and programs in biomedicine 165 (2018) 25–35.

[40] Z. Feng, J. Yang, L. Yao, Y. Qiao, Q. Yu, X. Xu, Deep retinal image segmentation: A fcn-based architecture with short and long skip connections for retinal image segmentation (2017) 713–722.

[41] V. Edupuganti, A. Chawla, A. Kale, Automatic optic disk and cup segmentation of fundus images using deep learning, in: 2018 25th IEEE International Conference on Image Processing (ICIP), IEEE, 2018, pp. 2227–2231.

[42] J. Tan, H. Fujita, S. Sivaprasad, S. Bhandary, A. Rao, K. Chua, U. Acharya, Automated segmentation of exudates, haemorrhages, microaneurysms using single convolutional neural network, Information sciences 420 (2017) 66–76.

[43] K. Maninis, J. Pont-Tuset, P. Arbeláez, L. Van Gool, Deep retinal image understanding, in: International Conference on Medical Image Computing and Computer-Assisted Intervention, Springer, 2016, pp. 140–148.

[44] G. Lim, Y. Cheng, W. Hsu, M. Lee, Integrated optic disc and cup segmentation with deep learning, in: Tools with Artificial Intelligence (ICTAI), 2015 IEEE 27th International Conference on, IEEE, 2015, pp. 162–169.

[45] S. Liu, S. Graham, A. Schulz, M. Kalloniatis, B. Zangerl, W. Cai, Y. Gao, B. Chua, H. Arvind, J. Grigg, et al., A deep learning-based algorithm identifies glaucomatous discs using monoscopic fundus photographs, Ophthalmology Glaucoma 1 (1) (2018) 15–22.

[46] A. Roy, S. Conjeti, S. Karri, D. Sheet, A. Katouzian, C. Wachinger, N. Navab, Relaynet: retinal layer and fluid segmentation of macular optical coherence tomography using fully convolutional networks, Biomedical optics express 8 (8) (2017) 3627–3642.

[47] L. Fang, D. Cunefare, C. Wang, R. Guymer, S. Li, S. Farsiu, Automatic segmentation of nine retinal layer boundaries in oct images of non-exudative amd patients using deep learning and graph search, Biomedical optics express 8 (5) (2017) 2732–2744.

[48] M. Pekala, N. Joshi, D. Freund, N. Bressler, D. DeBuc, P. Burlina, Deep learning based retinal oct segmentation, arXiv preprint arXiv:1801.09749.

[49] A. Ben-Cohen, D. Mark, I. Kovler, D. Zur, A. Barak, M. Iglicki, R. Soferman, Retinal layers segmentation using fully convolutional network in oct images, RSIP Vision.

[50] X. Liu, T. Fu, Z. Pan, D. Liu, W. Hu, J. Liu, K. Zhang, Automated layer segmentation of retinal optical coherence tomography images using a deep feature enhanced structured random forests classifier, IEEE journal of biomedical and health informatics.

[51] Y. Zhang, A. Chung, Deep supervision with additional labels for retinal vessel segmentation task, arXiv preprint arXiv:1806.02132.

[52] D. Maji, A. Santara, P. Mitra, D. Sheet, Ensemble of deep convolutional neural networks for learning to detect retinal vessels in fundus images, arXiv preprint arXiv:1603.04833.

[53] A. Oliveira, S. Pereira, C. Silva, Retinal vessel segmentation based on fully convolutional neural networks, Expert Systems with Applications.

[54] Z. Liu, Y. Zhang, P. Liu, Y. Zhang, Y. Luo, Y. Du, Y. Peng, P. Li, Retinal vessel segmentation using densely connected convolution neural network with colorful fundus images, Journal of Medical Imaging and Health Informatics 8 (6) (2018) 1300–1307.

[55] H. Leopold, J. Orchard, J. Zelek, V. Lakshminarayanan, Segmentation and feature extraction of retinal vascular morphology, in: Medical Imaging 2017: Image Processing, Vol. 10133, International Society for Optics and Photonics, 2017, p. 101330V.

[56] P. Liskowski, K. Krawiec, Segmenting retinal blood vessels with deep neural networks, IEEE transactions on medical imaging 35 (11) (2016) 2369–2380.

[57] H. Fu, Y. Xu, D. Wong, J. Liu, Retinal vessel segmentation via deep learning network and fully-connected conditional random fields, in: Biomedical Imaging (ISBI), 2016 IEEE 13th International Symposium on, IEEE, 2016, pp. 698–701.

[58] D. Maji, A. Santara, S. Ghosh, D. Sheet, P. Mitra, Deep neural network and random forest hybrid architecture for learning to detect retinal vessels in fundus images, in: Engineering in Medicine and Biology Society (EMBC), 2015 37th Annual International Conference of the IEEE, IEEE, 2015, pp. 3029–3032.

[59] J. Orlando, E. Prokofyeva, M. del Fresno, M. Blaschko, An ensemble deep learning based approach for red lesion detection in fundus images, Computer methods and programs in biomedicine 153 (2018) 115–127.

[60] M. van Grinsven, B. van Ginneken, C. Hoyng, T. Theelen, C. Sánchez, Fast convolutional neural network training using selective data sampling: application to hemorrhage detection in color fundus images, IEEE transactions on medical imaging 35 (5) (2016) 1273–1284.

[61] Y. Freund, H. Seung, E. Shamir, N. Tishby, Selective sampling using the query by committee algorithm, Machine learning 28 (2-3) (1997) 133–168.

[62] C. Lam, C. Yu, L. Huang, D. Rubin, Retinal lesion detection with deep learning using image patches, Investigative ophthalmology & visual science 59 (1) (2018) 590–596.

[63] J. Shan, L. Li, A deep learning method for microaneurysm detection in fundus images, in: Connected Health: Applications, Systems and Engineering Technologies (CHASE), 2016 IEEE First International Conference on, IEEE, 2016, pp. 357–358.

[64] M. Haloi, Improved microaneurysm detection using deep neural networks, arXiv preprint arXiv:1505.04424.

[65] F. Grassmann, J. Mengelkamp, C. Brandl, S. Harsch, M. Zimmermann, B. Linkohr, A. Peters, I. Heid, C. Palm, B. Weber, A deep learning algorithm for prediction of age-related eye disease study severity scale for age-related macular degeneration from color fundus photography, Ophthalmology.

[66] G. Ying, M. Maguire, J. Alexander, R. Martin, A. Antoszyk, Description of the age-related eye disease study 9-step severity scale applied to participants in the complications of age-related macular degeneration prevention trial, Archives of ophthalmology 127 (9) (2009) 1147–1151.

[67] A. Horta, N. Joshi, M. Pekala, K. Pacheco, J. Kong, N. Bressler, D. Freund, P. Burlina, A hybrid approach for incorporating deep visual features and side channel information with applications to amd detection, in: Machine Learning and Applications (ICMLA), 2017 16th IEEE International Conference on, IEEE, 2017, pp. 716–720.

[68] P. Burlina, K. Pacheco, N. Joshi, D. Freund, N. Bressler, Comparing humans and deep learning performance for grading amd: A study in using universal deep features and transfer learning for automated amd analysis, Computers in biology and medicine 82 (2017) 80–86.

[69] P. Sermanet, D. Eigen, X. Zhang, M. Mathieu, R. Fergus, Y. LeCun, Overfeat: Integrated recognition, localization and detection using convolutional networks, arXiv preprint arXiv:1312.6229.

[70] P. Burlina, N. Joshi, M. Pekala, K. Pacheco, D. Freund, N. Bressler, Automated grading of age-related macular degeneration from color fundus images using deep convolutional neural networks, JAMA ophthalmology 135 (11) (2017) 1170–1176.

[71] A. Govindaiah, M. Hussain, R. Smith, A. Bhuiyan, Deep convolutional neural network based screening and assessment of age-related macular degeneration from fundus images, in: Biomedical Imaging (ISBI 2018), 2018 IEEE 15th International Symposium on, IEEE, 2018, pp. 1525–1528.

[72] S. Matsuba, H. Tabuchi, H. Ohsugi, H. Enno, N. Ishitobi, H. Masumoto, Y. Kiuchi, Accuracy of ultra-wide-field fundus ophthalmoscopy-assisted deep learning, a machine-learning technology, for detecting age-related macular degeneration, International ophthalmology (2018) 1–7.

[73] J. Tan, S. Bhandary, S. Sivaprasad, Y. Hagiwara, A. Bagchi, U. Raghavendra, A. Rao, B. Raju, N. Shetty, A. Gertych, et al., Age-related macular degeneration detection using deep convolutional neural network, Future Generation Computer Systems 87 (2018) 127–135.

[74] D. Kingma, J. Ba, Adam: A method for stochastic optimization, arXiv preprint arXiv:1412.6980.

[75] M. Treder, J. Lauermann, N. Eter, Automated detection of exudative age-related macular degeneration in spectral domain optical coherence tomography using deep learning, Graefe's Archive for Clinical and Experimental Ophthalmology 256 (2) (2018) 259–265.

[76] D. Kermany, M. Goldbaum, W. Cai, C. Valentim, H. Liang, S. Baxter, A. McKeown, G. Yang, X. Wu, F. Yan, et al., Identifying medical diagnoses and treatable diseases by image-based deep learning, Cell 172 (5) (2018) 1122–1131.

[77] R. Asaoka, H. Murata, A. Iwase, M. Araie, Detecting preperimetric glaucoma with standard automated perimetry using a deep learning classifier, Ophthalmology 123 (9) (2016) 1974–1980. `doi:10.1016/j.ophtha.2016.05.029`.

[78] L. Zhixi, Y. He, S. Keel, W. Meng, R. Chang, M. He, Efficacy of a deep learning system for detecting glaucomatous optic neuropathy based on color fundus photographs, Ophthalmology 125 (8) (2018) 1199–1206. `doi:10.1016/j.ophtha.2018.01.023`.

[79] C. Xiangyu, X. Yanwu, W. Damon, W. Tien, L. Jiang, Glaucoma detection based on deep convolutional neural network. (Aug 2015). URL `https://www.ncbi.nlm.nih.gov/pubmed/26736362/`

[80] X. Chen, Y. Xu, S. Yan, D. Wong, T. Wong, J. Liu, Automatic feature learning for glaucoma detection based on deep learning (Oct 2015). URL `https://link.springer.com/chapter/10.1007/978-3-319-24574-4_80`

[81] Y. Chai, H. Liu, J. Xu, Glaucoma diagnosis based on both hidden features and domain knowledge through deep learning models, Knowledge-Based Systems`doi:10.1016/j.knosys.2018.07.043`.

[82] H. Fu, J. Cheng, Y. Xu, C. Zhang, D. Wong, J. Liu, X. Cao, Disc-aware ensemble network for glaucoma screening from fundus image, IEEE Transactions on Medical Imaging.

[83] A. Chakravarty, J. Sivswamy, A deep learning based joint segmentation and classification framework for glaucoma assesment in retinal color fundus images, arXiv preprint arXiv:1808.01355.

[84] H. Muhammad, T. Fuchs, N. De Cuir, C. De Moraes, D. Blumberg, J. Liebmann, R. Ritch, D. Hood, Hybrid deep learning on single wide-field optical coherence tomography scans accurately classifies glaucoma suspects, Journal of glaucoma 26 (12) (2017) 1086–1094.

[85] H. Fu, Y. Xu, S. Lin, D. Wong, B. Mani, M. Mahesh, T. Aung, J. Liu, Multi-context deep network for angle-closure glaucoma screening in anterior segment oct, in: International Conference on Medical Image Computing and Computer-Assisted Intervention, Springer, 2018, pp. 356–363.

[86] G. C. Chan, R. Kamble, H. Müller, S. Shah, T. Tang, F. Mériaudeau, Fusing results of several deep learning architectures for automatic classification of normal and diabetic macular edema in optical coherence tomography, in: 2018 40th Annual International Conference of the IEEE

Engineering in Medicine and Biology Society (EMBC), IEEE, 2018, pp. 670–673.

[87] A. Vahadane, A. Joshi, K. Madan, T. Dastidar, Detection of diabetic macular edema in optical coherence tomography scans using patch based deep learning, in: Biomedical Imaging (ISBI 2018), 2018 IEEE 15th International Symposium on, IEEE, 2018, pp. 1427–1430.

[88] A. Varadarajan, P. Bavishi, P. Raumviboonsuk, P. Chotcomwongse, S. Venugopalan, A. Narayanaswamy, J. Cuadros, K. Kanai, G. Bresnick, M. Tadarati, et al., Predicting optical coherence tomography-derived diabetic macular edema grades from fundus photographs using deep learning, arXiv preprint arXiv:1810.10342.

[89] O. Perdomo, S. Otálora, F. González, F. Meriaudeau, H. Müller, Octnet: A convolutional network for automatic classification of normal and diabetic macular edema using sd-oct volumes, in: Biomedical Imaging (ISBI 2018), 2018 IEEE 15th International Symposium on, IEEE, 2018, pp. 1423–1426.

[90] R. Gargeya, T. Leng, Automated identification of diabetic retinopathy using deep learning, Ophthalmology 124 (7) (2017) 962–969.

[91] H. Takahashi, H. Tampo, Y. Arai, Y. Inoue, H. Kawashima, Applying artificial intelligence to disease staging: Deep learning for improved staging of diabetic retinopathy, PloS one 12 (6) (2017) e0179790.

[92] E. Colas, A. Besse, A. Orgogozo, B. Schmauch, N. Meric, E. Besse, Deep learning approach for diabetic retinopathy screening, Acta Ophthalmologica 94.

[93] G. García, J. Gallardo, A. Mauricio, J. López, C. Del Carpio, Detection of diabetic retinopathy based on a convolutional neural network using retinal fundus images, in: International Conference on Artificial Neural Networks, Springer, 2017, pp. 635–642.

[94] M. Abràmoff, Y. Lou, A. Erginay, W. Clarida, R. Amelon, J. Folk, M. Niemeijer, Improved automated detection of diabetic retinopathy on a publicly available dataset through integration of deep learning, Investigative ophthalmology & visual science 57 (13) (2016) 5200–5206.

[95] J. Brown, J. Campbell, A. Beers, K. Chang, S. Ostmo, R. Chan, J. Dy, D. Erdogmus, S. Ioannidis, J. Kalpathy-Cramer, et al., Automated diagnosis of plus disease in retinopathy of prematurity using deep convolutional neural networks, JAMA ophthalmology.

[96] V. Gulshan, L. Peng, M. Coram, M. Stumpe, D. Wu, A. Narayanaswamy, S. Venugopalan, K. Widner, T. Madams, J. Cuadros, et al., Development and validation of a deep learning algorithm for detection of diabetic retinopathy in retinal fundus photographs, Jama 316 (22) (2016) 2402–2410.

[97] G. Quellec, K. Charrière, Y. Boudi, B. Cochener, M. Lamard, Deep image mining for diabetic retinopathy screening, Medical image analysis 39 (2017) 178–193.

[98] https://www.kaggle.com/c/diabetic-retinopathy-detection/discussion/15617.

[99] Z. Zhang, R. Srivastava, H. Liu, X. Chen, L. Duan, D. K. Wong, C. Kwoh, T. Wong, J. Liu, A survey on computer aided diagnosis for ocular diseases, BMC medical informatics and decision making 14 (1) (2014) 80.

[100] P. Teikari, R. Najjar, L. Schmetterer, D. Milea, Embedded deep learning in ophthalmology: Making ophthalmic imaging smarter, arXiv preprint arXiv:1810.05874.

[101] E. Rahimy, Deep learning applications in ophthalmology, Current opinion in ophthalmology 29 (3) (2018) 254–260.

[102] D. Hogarty, D. Mackey, A. Hewitt, Current state and future prospects of artificial intelligence in ophthalmology: a review, Clinical & experimental ophthalmology.

[103] H. Leopold, J. Orchard, J. Zelek, V. Lakshminarayanan, Pixelbnn: Augmenting the pixelcnn with batch normalization and the presentation of a fast architecture for retinal vessel segmentation, arXiv preprint arXiv:1712.06742.

[104] M. Wang, W. Deng, Deep visual domain adaptation: A survey, Neurocomputing.

Sourya Sengupta is a first year student pursuing dual degree in Vision Science and System Design Engineering in University of Waterloo. He completed his B.E. in Electrical Engineering from Jadavpur University, Kolkata. His research interest includes Deep Learning Application in Medical Imaging.

Amitojdeep Singh is a final year student pursuing dual majors in BE Computer Science and MSc Economics from Birla Institute of Technology and Science, Pilani, India. His research interest is in application of Deep Learning in computer vision and biomedical imaging.

Henry A. Leopold is a Doctoral candidate at the University of Waterloo in the department of systems design engineering, joint with vision science through the school of optometry. He received his BASc in materials science bioengineering from the University of Toronto in 2010. He has worked in molecular disease research, public health surveillance and entrepreneurial industries. His current research interests include artificial intelligence, biomedical informatics, cybernetics and implant engineering.

Vasudevan Lakshminarayanan is a Professor at University of Waterloo. He received his Ph.D. in Physics from the University of California at Berkeley and is a Fellow of SPIE, OSA, APS, AAAS, etc. He serves on the optics advisory board of the Abdus Salam International Center for Theoretical Physics in Trieste, Italy. He has published widely in various areas including physics, neuroscience, bioengineering, applied math.